
[View Journal Online](#)  
[View Article Online](#)

# A review on polymer nanocomposite hydrogel preparation, characterization, and applications

 Md. Arif Roman Azady <sup>1</sup>, Sony Ahmed <sup>2</sup>, and Md. Shafiul Islam <sup>1,3,\*</sup>
<sup>1</sup> Department of Applied Chemistry and Chemical Engineering, Noakhali Science and Technology University, Noakhali, 3814, Bangladesh  
[romanazady@gmail.com](mailto:romanazady@gmail.com) (M.A.R.A.)

<sup>2</sup> Faculty of Science and Marine Environment, Universiti Malaysia Terengganu, Terengganu, 21030, Malaysia  
[sonyahmed91@gmail.com](mailto:sonyahmed91@gmail.com) (S.A.)

<sup>3</sup> Department of Chemistry, Virginia Commonwealth University, Richmond, 23223, United States  
[shafiulacce@gmail.com](mailto:shafiulacce@gmail.com) (M.S.I.)

 \* Corresponding author at: Department of Chemistry, Virginia Commonwealth University, Richmond, 23223, United States.  
 e-mail: [shafiulacce@gmail.com](mailto:shafiulacce@gmail.com) (M.S. Islam).

## REVIEW ARTICLE



doi 10.5155/eurjchem.12.3.329-339.2100

 Received: 30 January 2021  
 Received in revised form: 27 March 2021  
 Accepted: 03 April 2021  
 Published online: 30 September 2021  
 Printed: 30 September 2021

## KEYWORDS

 Hydrogel  
 Gel content  
 X-ray diffraction  
 Adsorption study  
 Nanocomposite hydrogel  
 Thermogravimetric analysis

## ABSTRACT

Nanocomposite hydrogels, made by incorporating nanoparticles into a hydrogel matrix, have been developed to fulfill the need for materials with enhanced and predictable mechanical properties and functionality. This review breaks down the process of preparing and characterizing nanocomposite hydrogels and looks at the various applications they can be used for. Through careful selection of the nanoparticle and hydrogel types, as well as the preparation method, the degree of crosslinking and the strength of the intermolecular interactions between the nanoparticles and the hydrogel matrix can be controlled. Once the nanomaterial is prepared, the morphology, gel content, thermal stability, and mechanical properties are investigated. By varying the concentrations of nanoparticles within the hydrogel matrix, nanocomposite hydrogels with optimal functionality and mechanical properties are produced. The optimized nanomaterial can then be used for its intended application(s); here the focus is on applications in the biomedical and dye adsorption fields. With further research, it is predicted that nanocomposite hydrogels will fulfill their potential to be used in practical, everyday applications.

 Cite this: *Eur. J. Chem.* 2021, 12(3), 329-339

 Journal website: [www.eurjchem.com](http://www.eurjchem.com)

## 1. Introduction

A hydrogel is made of a three-dimensional (3D) network of polymers containing hydrophilic and hydrophobic parts in a defined proportion. When placed in aqueous medium, hydrogels can swell, increasing their initial volume by at least 10% without breaking down or significantly changing their shape. This swelling ability is due to the crosslinking between the polymer chains of the hydrogel, which allows the hydrogel to swell and shrink [1-3]. The functionality and wettability of a hydrogel largely depends on the type of functional groups attached to the monomers used to form the polymer backbone of the hydrogel [4]. For example, hydrophilic functional groups create an osmotic pressure gradient, allowing water to diffuse into the hydrogel through a capillary action, making it swell. The swelling ability can be controlled through the polymerization method and chemical properties of the incorporated nanoparticles [5]. Hydrogels have been used in a diverse range of hygienic, agricultural, medical, and pharmaceutical applications because they are hydrophilic, biocompatible, and relatively nontoxic. In such applications, the water absorbency and

water retention properties are essential [6]. Therefore, hydrogels have interesting applications in tissue engineering [7], drug delivery [8], chemical sensing and biosensing [9], and separation and purification technologies [10], to name a few. Recently, polymeric hydrogels have attracted much scientific interest and have found uses in many fields [11], including molecular filters [12,13], superabsorbents [14], and contact lenses [15].

Conventional hydrogels have relatively poor mechanical properties and limited functions arising from their soft and fragile nature, hampering their usefulness in practical applications [16]. To overcome these issues, many researchers have focused on creating hydrogels with higher mechanical performances by creating thin layers or small particles [17-19], using cold-treatment [20], introducing macro- or nano-porous structures [21,22], grafting polymers by adding hydrophobic crosslinkers [23], using hydrophilic silica as nanosized water reservoirs or preparing gels in organic/water mixture media [24,25], sliding hydrogels [26], forming double-network hydrogels [27], using figure-of-eight crosslinkers to make topological gels (TP gel) [28], and creating nanocomposite (NC)

hydrogels [29]. Recently, organic nanoparticles (NPs) [30], interpenetrating polymer network [31-33], and inorganic NP composite hydrogels [34,35] with enhanced functionality were prepared to broaden the spectrum of applications of hydrogels [36]. Compared with other materials, NC hydrogels have the advantages of ease of preparation and usually enhanced mechanical properties, owing to their unique microstructure network of flexible polymer chains physically crosslinked by homogeneously dispersed inorganic NPs. Unfortunately, only a few types of inorganic NPs, including clay [37], graphene oxide [38], calcium hydroxide spherulite [39], and layered double hydroxides (LDHs) [40], have been successfully employed to achieve NC hydrogels. Multiple functions of NC hydrogels, such as photoluminescence (PL), remain a great challenge, although NC hydrogels with enhanced mechanical properties have been extensively studied. Considering the high photochemical stability, sharp emission bands, and low toxicity of rare-earth (RE) elements [41,42], luminescent polymer hydrogels containing two or more active RE ions are ideal candidates to offer multi-color PL emissions by simply changing the relative ratios of RE ions [43,44].

Nanocomposite hydrogels are prepared from the combination of polymers and NPs by chemical or physical interactions [45,46]. Examples of functional NPs include metal/metal oxide NPs, polymeric NPs, silica NPs, semiconductor quantum dots, and carbon-based nanomaterials (Graphene oxide, carbon nanotubes, and NCs) [47]. The resulting hydrogels have increased functionality and interesting applications in the fields of sensing [48], actuators [49], biomedicine [50], separation and purification technologies [51], and computing [52].

Polymeric NC materials are being used as an alternative for conventional polymeric materials because they are lightweight and inexpensive, with excellent physicochemical properties [53]. Attempts are being made to fabricate a greater variety of polymeric NCs and to understand their fundamental principles to make them applicable in different areas of science and engineering. By incorporating nanocomposite fillers into the polymer matrix, many of the properties of the polymer, such as the structural, optical, and electrical properties, can be tuned [54,55]. Various types of polymers (polyethylene, polyvinylidene fluoride, polypropylene, polymethyl methacrylate, polyaniline, polyvinyl chloride, polyamide, polyethylene terephthalate, polystyrene, etc.) loaded with different types of nanofillers (CuO, ZnO, ZnS, CuS, CdSe, Cds, GO, FeO, etc.) have been used to fabricate polymeric NCs with enhanced structural, optical, mechanical, and electrical properties [53,56].

## 2. Preparation of nanocomposite hydrogels

NC hydrogels are an important chapter in hydrogel conception. The preparation of NC hydrogels is similar to that of conventional hydrogels. Here, we discuss some methods for the preparation of NC hydrogels. It is simple to prepare NC hydrogels by gelation, which is mostly driven by electrostatic interactions and hydrogen bonding between the NCs and polymer chains [57]. One NC hydrogel prepared by gelation is made from polyethyleneimine (PEI), microcrystalline cellulose, and carbon dots (CDs). This NC hydrogel forms due to the strong hydrogen bonding that occurs between the cellulose and PEI-CDs [58]. A similar NC hydrogel prepared by gelation is a chitosan/CD NC hydrogel film, where the electrostatic interaction between the oppositely charged chitosan and CDs drives the formation of the hydrogel [59]. NC hydrogels have also been prepared by first radically polymerizing [2-(acryloyloxy)ethyl]trimethylammonium chloride (AETA) with *N,N'*-methylenebisacrylamide (MBA) as a crosslinker, then immersing the dried cationic polymer network in an aqueous graphene quantum dot suspension [60].

NC hydrogels are often formed by the *in-situ* polymerization of a mixed solution of polymerizable monomers and NCs [61],

such as acrylamide (AM) in a suspension of CDs [62]. Recently, a fluorescent waveguide NC hydrogel was created by photopolymerizing a mixture of CDs and a hydrogel precursor [63]. Additionally, the photopolymerization of an aqueous solution of *N*-methacryloyl chitosan and NCs produced an injectable NC hydrogel [64]. NC hydrogels have also been formed by mixing NCs directly into polymers. A cyclic freezing-thawing process was recently used, where NC hydrogel pipes were prepared by loading montmorillonite (MMT) into a polyvinyl alcohol (PVA) matrix [65]. Another NC hydrogel made with this method was comprised of nano-ZnO loaded in poly(*N*-isopropylacrylamide-co-acrylic acid) (P(NIPAm-co-AAc)) using an *in-situ* process [66].

The self-assembly method is another method which is effective for making NC-based hydrogels. Recently, it was used for the preparation of a 3D graphene-based hydrogel (GBH), which self-assembles via  $\pi$ - $\pi$  interactions of graphene oxide (GO) sheets [67]. Other self-assembly methods have been developed for 3D GBHs, such as hydrothermal processes [68], chemical reduction [69], and metal ion-induced processes [70]. Another method, which takes advantage of the ability of GO to disperse in polar solvents, is the mixed solution method. It has been used to prepare a graphene/gelatin hydrogel composite film that exhibits improved tensile strength over pure gelatin films [71]. The mixed solution method has also been used to produce Au-NP hydrogel composites, which are formed by adding Silica-Au nanoshells to a monomer solution with a gel initiator, crosslinker, and accelerator [72]. An additional way of preparing NC hydrogels is via the physical incorporation of NPs into a hydrogel matrix after gel formation, such as by immersing electropolymerized polyacrylamide (PAAm) gel into an Au-NP solution [73]. A final method of creating NC hydrogels is by using NPs, like clay or titanate nanosheets (clay-NSs or TiNSs), as crosslinkers, which results in NC hydrogels with enhanced mechanical properties [47,74].

## 3. Characterization

### 3.1. Gel content

To determine the gel content, the hydrogel samples are first dried to a constant weight, then immersed overnight in room temperature distilled water to remove any impurities. After soaking overnight, the gel samples were oven-dried to a constant weight. The gel fractions of the samples were calculated according to the method of Khoylou *et al.* [75] as follows:

$$\text{Gel fraction (\%)} = \frac{W_d}{W_i} \times 100 \quad (1)$$

where  $W_d$  is the dry weight of the gel after impurity extraction and  $W_i$  is the initial weight of the dried gel. Measuring the weight after vacuum filtration results in a more accurate measure of the insoluble fraction, or the hydrogel. The gel fraction, calculated by using the initial weight of dry gel ( $W_0$ ) and the weight of extracted dry gel ( $W_i$ ) according to the following equations [76,77]:

$$\text{Sol fraction (\%)} = \frac{W_0 - W_i}{W_i} \times 100 \quad (2)$$

$$\text{Gel fraction (\%)} = 100 - \text{Sol fraction\%} \quad (3)$$

### 3.2. Determination of swelling ratio

The swelling ratio is the percent of change in hydrogel weight as a result of water absorption over time. Experimentally, a sample of preweighed, dry hydrogel is immersed in distilled water, then taken from the water at regular time intervals and weighed after removing the surface water. Finally, the percent of swelling of each sample is calculated using the

weight of the swollen gel at time  $t$ , ( $W_t$ ) and the initial weight of the dry gel ( $W_i$ ) according to the following equation [78,79],

$$\text{Percent Swelling (\%)} = \frac{W_t - W_0}{W_0} \times 100\% \quad (4)$$

The equilibrium swelling ratio (ESR) is the maximum amount of water able to be absorbed by gel samples and is determined by using the weight of the swollen gel at equilibrium ( $W_s$ ) and  $W_0$  according to the following equation [80],

$$\text{ESR} = \frac{W_s - W_0}{W_0} \quad (5)$$

The ESR of polymer gels is important to water shut-off treatments and is related to the salt sensitivity factor,  $f$ , which represents the ratio of the polymer's ESRs in tap water (ESR) and in aqueous electrolyte solution (ESR<sub>e</sub>), according to the following equation [81].

$$f = 1 - \frac{\text{ESR}_e}{\text{ESR}} \quad (6)$$

For NC hydrogels prepared with sodium montmorillonite (Na-MMT) and sulfonated polyacrylamide (PAMPS), increasing the concentration of Na<sup>+</sup>-MMT from 0 ppm to 4000 ppm caused a decrease in ESR and  $f$  [82]. This may be related to trapped Na<sup>+</sup>-MMT being unable to contribute to the osmotic pressure of the hydrogel, which is the main cause of gel swelling. Another explanation for the decrease in ESP and  $f$  may be the increase of crosslinked points in the polymeric network, decreasing the hydrogel's ability to swell. This result also confirmed that the  $f$  factors for NC hydrogels are slightly lower than those for traditional hydrogels because the NC hydrogels had decreased copolymer mobility chains within their network and, as such, had low  $f$  factor amounts whilst their ability to swell was more appropriate. The swelling capacity of saponite + PAAm hydrogels is greater than that of conventional PAAm hydrogels, which is likely due to hydrogen bonding between the absorbed water and the NH<sub>2</sub> group of the saponite [16]. For the PVA/MMT NC hydrogel pipes loaded with 10 wt % MMT, the ESR after 6 hours of drying was reduced by 25%. This may also be attributed to the increased crosslinking restricting the absorption of water molecules during the swelling processes [65].

### 3.3. Surface morphology study

Scanning electron microscopy (SEM) is used to characterize the surface morphology of NC hydrogel samples, which changes with the addition of NPs [83]. For the NC hydrogels made by the in-situ polymerization of organo-MMT and *N*-isopropylacrylamide (NIPAAm), SEM images show that as the concentration of organo-MMT increases, the pore size decreases. This reduction is likely a result of the increased number of crosslinked points as a function of the increased concentration of organo-MMT [84]. Figure 1, A/II, B/II, C/II, and D/II indicates the decreasing pore size of the organo-MMT/PNIPAAm NC hydrogel as a function of the increasing organo-MMT concentration. The PVA/MMT NC hydrogel pipes also showed a decreasing pore size with increasing MMT levels, which was determined to have resulted from increased crosslinking within the hydrogel matrix [65]. SEM was also used to show the effect of Na-MMT addition on the pore size of PVA hydrogels. As with the other MMT-loaded NC hydrogels, the pore diameter was shown to decrease with increased MMT concentration [85]. Decreasing pore size with increasing nanoparticle concentration is a continuous trend across other nanoparticle/hydrogel combinations, including multiwalled carbon nanotubes (MCNTs) incorporated into  $\kappa$ -carageenan hydrogels, as shown in Figure 2 [86].

It was found that the surface of a conventional sodium carboxymethylcellulose (CMC-Na)/PVA-based hydrogel was almost smooth; however, the surface morphology changed to a more wrinkled appearance after the addition of cellulose nanocrystals (CNCs). Even the distribution of CNCs in the hydrogel improves its thermal and mechanical properties [87]. In the SEM images of the saponite + PAAm hydrogel shown in Figure 3a, a smooth surface with embedded clay particles can be observed. This hydrogel was then used to develop AgO NPs within the NC hydrogel matrix. The silver loaded hydrogel is shown in Figure 3b, while the AgO NPs incorporated into the hydrogel matrix are shown in Figure 3c [16].

### 3.4. X-ray diffraction pattern analysis

X-ray diffraction (XRD) is used to understand how nanoparticles develop in hydrogel networks. It has often been used to assess the morphology of prepared nanocomposite hydrogels [88]. In particular, the interactions between bioactive molecules and nanocarriers (including organic/inorganic nanoparticles, small bioorganic molecules, and polymers) and the organizational phase of such nanocarriers in NC hydrogels have been thoroughly documented via small-angle X-ray scattering (SAXS) and XRD [89]. Pure organic polymer hydrogels like PAAm cannot be detected with XRD because they are amorphous; instead, they exhibit peaks of confusion. When NPs like halloysite nanotubes (HNTs) are added to polymeric hydrogels like PAAm, the diffraction peaks of the hydrogel sample and its nanocomposites are changed, shifting to reflect the strength of the interactions between the polymer chains and the NPs [90]. The XRD pattern of the saponite and PAAm hydrogel shows a characteristic diffraction peak at 24.29°. When AgO NPs are developed in the hydrogel matrix, the diffraction pattern develops peaks corresponding to face-centered cubic silver, as shown in Figure 4 [16].

In the MMT/PVA NC hydrogel pipes, there was no distinct diffraction peak and the diffraction peak associated with MMT had been removed (Figure 5) [65]. This confirmed crosslinking between the PVA and the MMT and the formation of a homogenous NC hydrogel.

### 3.5. Mechanical properties of nanocomposite hydrogels

Conventional hydrogels, prepared by copolymerization of one or more functional monomers in the presence of a cross-linker, have been of great interest due to their applications in agriculture [91], drilling fluids [92], tissue engineering [93,94], and waste treatment [95]. However, highly swollen hydrogels are usually very fragile due to a lack of efficient energy dissipation mechanics, which has restricted the further growth of traditional hydrogels. Recently, efforts have been made to improve their mechanical strength, with some solutions including the addition of nanoparticles to tune the properties of the resulting hydrogel. These NC hydrogels exhibit enhanced mechanical properties, such as high tensile strength, and can withstand extensive deformations, like stretching, compression, tearing, and knotting (Figure 6) [96,97].

The total stretched length of an NC gel can vary to over 1000%, depending on the type of NP and polymer used. NC hydrogels like poly(*N,N*-dimethylacrylamide) (PDMAA-NC) crosslinked with synthetic hectorite can stretch to 1600% of its original length [98]. Tensile testing can be used to measure the impact of NP addition to conventional hydrogels. Incorporating increasing concentrations of HNTs into the PAAm hydrogel matrix results in NC hydrogels with nearly linearly increasing limits of stretching ability [90].

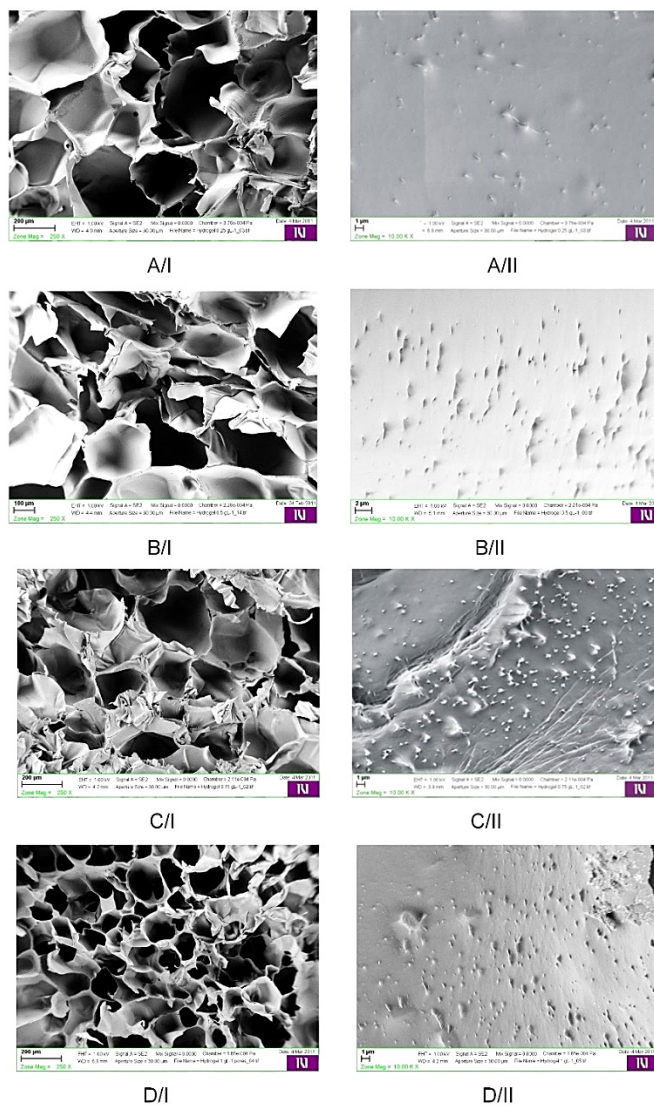


**Figure 1.** Surface morphology of MMT-loaded NC hydrogels, with loading concentration increasing from (A): 0.25% MMT to (D): 1% MMT [84].

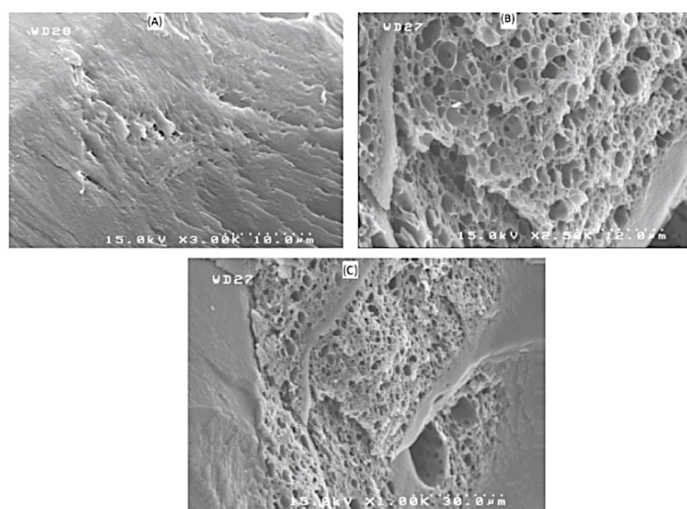


**Figure 2.** Surface morphology of (A)  $\kappa$ -carrageenan, (B) pure  $\kappa$ -carrageenan hydrogel, and (c) MCNT-loaded NC hydrogel. Licensed under CC-BY-NC-ND 3.0 [86].

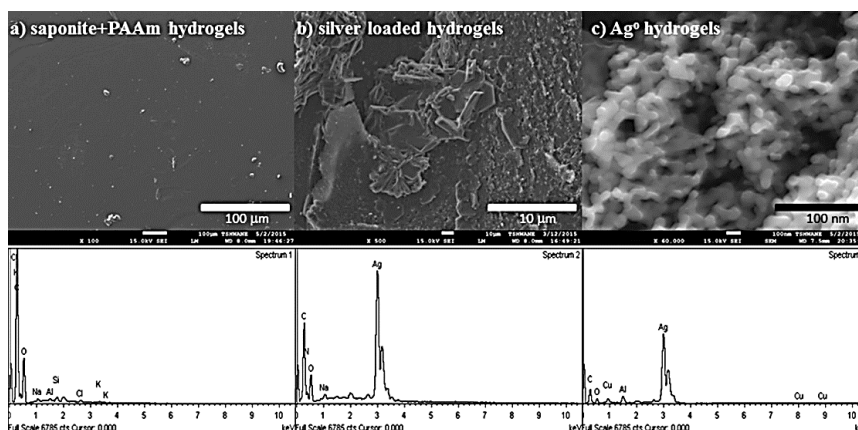


**Figure 3.** Surface morphology and respective EDS spectra of (a) saponite + PAAm hydrogel, (b) silver-loaded hydrogel and (c) AgO NC hydrogel. Copyright (2016) Wiley. Used with permission from (Bandla, Silver nanoparticles incorporated within intercalated clay/polymer nanocomposite hydrogels for antibacterial studies, *Polym. Compos.*) [16].

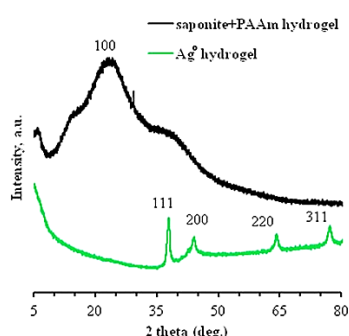


**Figure 4.** XRD spectra of saponite + PAAm hydrogel and AgO-NC hydrogel. Copyright (2016) Wiley. Used with permission from (Bandla, Silver nanoparticles incorporated within intercalated clay/polymer nanocomposite hydrogels for antibacterial studies, *Polym. Compos.*) [16].

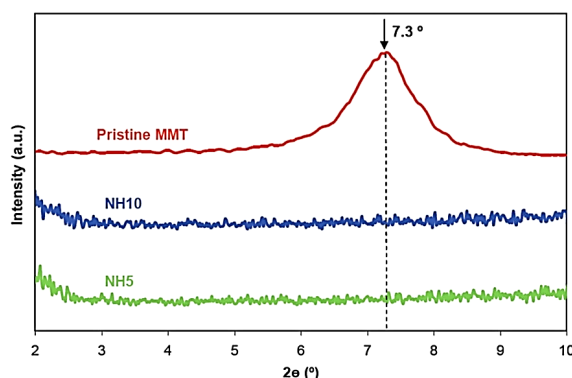


**Figure 5.** XRD spectra of MMT/PVA NC hydrogel pipes containing 0% (pristine), 5% (NH5), or 10% (NH10) of MMT. Copyright (2019) Wiley. Used with permission from (Sirousazar, Polymer-clay nanocomposite hydrogels for molecular irrigation application, *J. Appl. Polym. Sci.*) [65].

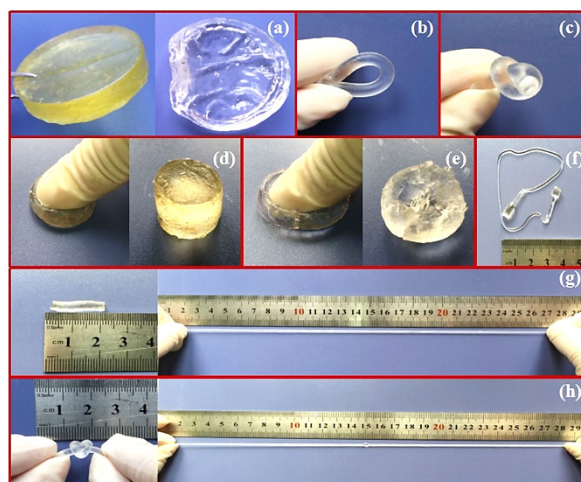
When CNCs are used as a strengthening filler in carboxymethyl cellulose (CMC), the tensile strength of the composite is 17% higher than that of pure CMC. Additionally, the tensile modulus of the CNC NC hydrogel is 60%, which is higher than that of pure CMC. Microcrystalline cellulose (MCC) was also added to the CMC matrix but was proven not to increase tensile strength or tensile modulus [99]. PVA/MMT NC hydrogels made with increasing concentrations of Na-MMT have been shown to have nearly linearly increasing tensile strength and tensile modulus (Figure 7) [65].

Compression stress-strain curves for polyacrylamide (PAM), PAM/chitosan nanofibers (PAM-CNFs), and PAM-CNF semi-interpenetrating polymer networks (PAM-SIPNs) show that the compression strength and storage modulus of the PAM-CNFs and PAM-SIPNs is higher than those of the pure PAM

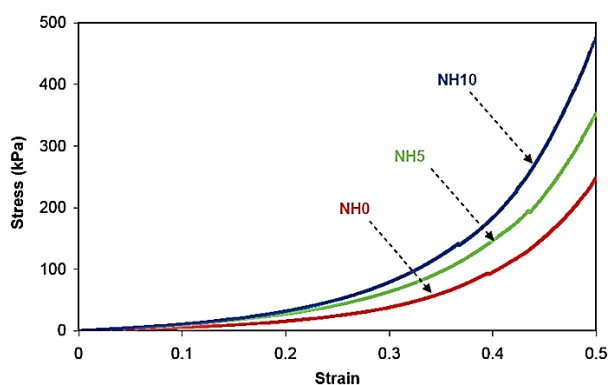
hydrogels, with PAM-CNF having the greatest values [100]. An interesting NC hydrogel, termed an organic NC PAAm hydrogel (OC gel), which is crosslinked with polystyrene (PS), showed generally increased tensile strength up to a PS concentration of 40%, with an optimal tensile strength at a PS concentration of 10% [30].

### 3.6. Thermogravimetric analysis

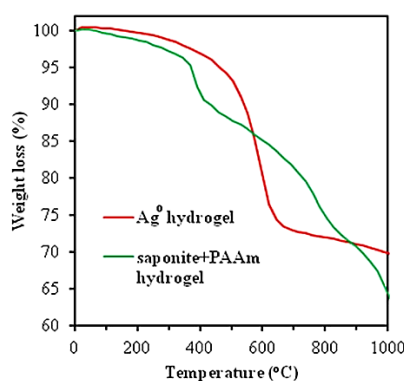
Thermogravimetric analysis (TGA) is a heat analysis tool in which the temperature of the sample is steadily increased, causing corresponding changes in the mass of the sample over time [101]. Therefore, it is an effective tool to understand the thermal events of NC hydrogels when they are heated at a fixed rate [102].



**Figure 6.** NC gels undergoing rigorous mechanical testing: (a) WSCA/PAM NC hydrogel (left) compared to pure PAM hydrogel (right); NC hydrogel being (b) bent, (c) knotted, and (d) compressed/decompressed; PAM hydrogel being (e) compressed/decompressed and (f) stretched; NC hydrogel being (g) stretched and (h) stretched while knotted. Licensed under CC-BY 4.0 [96].



**Figure 7.** Compressive stress–strain curves of MMT/PVA NC hydrogel pipes containing 0% (NH0), 5% (NH5), or 10% (NH10) MMT. Copyright (2019) Wiley. Used with permission from (Sirousazar, Polymer-clay nanocomposite hydrogels for molecular irrigation application, *J. Appl. Polym. Sci.*) [65].



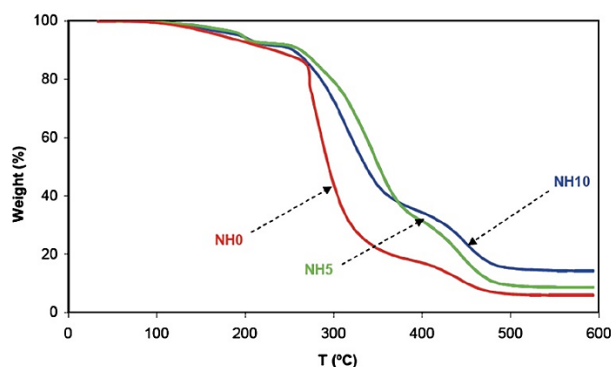
**Figure 8.** TGA of saponite + PAAM hydrogel and AgO-NC hydrogel. Copyright (2016) Wiley. Used with permission from (Bandla, Silver nanoparticles incorporated within intercalated clay/polymer nanocomposite hydrogels for antibacterial studies, *Polym. Compos.*) [16].

Figure 8 shows a thermogram of the NC hydrogel made by crosslinking saponite and PAAM, as well as the hydrogel after growing Ag NPs in the hydrogel matrix. The thermogram shows that the AgO-NC hydrogel is stable over a greater temperature range than the original saponite + PAAM NC hydrogel [16].

Figure 9 shows a thermogram of the PVA/MMT NC hydrogels prepared by the cyclic freezing-thawing method, where the number at the end of the sample name indicates the percentage of MMT in the hydrogel matrix. The NH0 degradation temperature peaks were observed at lower tempera-

tures than the NH5 and NH10 degradation peaks, suggesting that the addition of MMT into the PVA hydrogel matrix improves the thermal stability of the hydrogel [65].

Thermograms of PAM, PAM-CNF, and PAM-SIPN show three degradation stages, corresponding to the loss of water under 250 °C, the loss of an NH<sub>2</sub> group between 250 and 320°C, and the degradation of the polymer chains above 320°C. These results show that the thermal stability of PAM-CNF and PAM-SIPN are only slightly greater than those of the original PAM hydrogel [100].



**Figure 9.** TGA analysis of MMT/PVA NC hydrogel pipes containing 0% (NH0), 5% (NH5), or 10% (NH10) MMT Copyright (2019) Wiley. Used with permission from (Sirousazar, Polymer-clay nanocomposite hydrogels for molecular irrigation application, *J. Appl. Polym. Sci.*) [65].

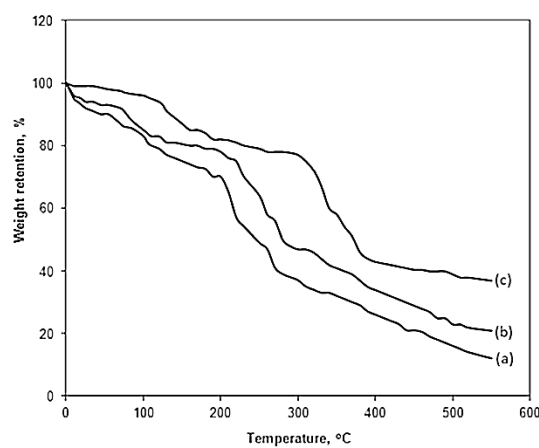


**Figure 10.** TGA analysis of (a)  $\kappa$ -carrageenan, (b) pure  $\kappa$ -carrageenan hydrogel, and (c) MCNT-loaded NC hydrogel. Licensed under CC-BY-NC-ND 3.0 [86].

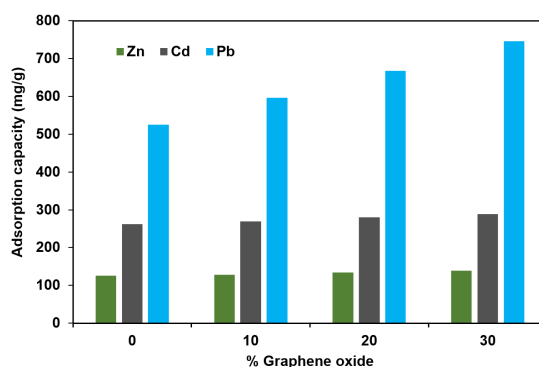


**Figure 11.** The influence of GO nanoparticle addition on the metal ion adsorption capacity of xylan-g-/P(AA-co-AM) hydrogels.

Figure 10 shows that the initial degradation temperature of the MCNT-loaded  $\kappa$ -carrageenan NC hydrogel is significantly higher than that of the pure hydrogel, thus indicating the NC hydrogel's increased thermal stability [86]. For NC hydrogels made with sodium alginate-g-polyacrylic acid polymerized with  $\text{TiO}_2$  (SA-g-PAA/ $\text{TiO}_2$ ), the degradation curves of the NC hydrogel are slightly more thermally stable than the original SA-g-PAA hydrogel, indicating that  $\text{TiO}_2$  may act as a thermal barrier for the SA-g-PAA polymer chains [103].

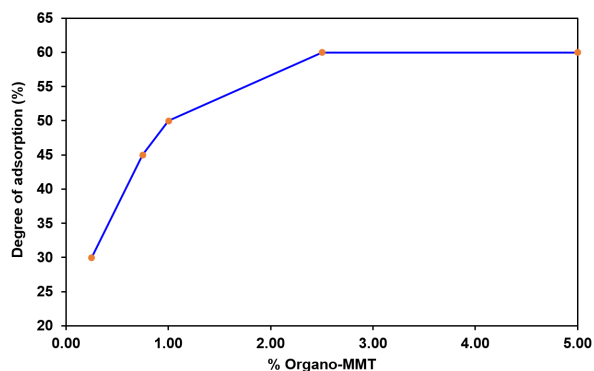
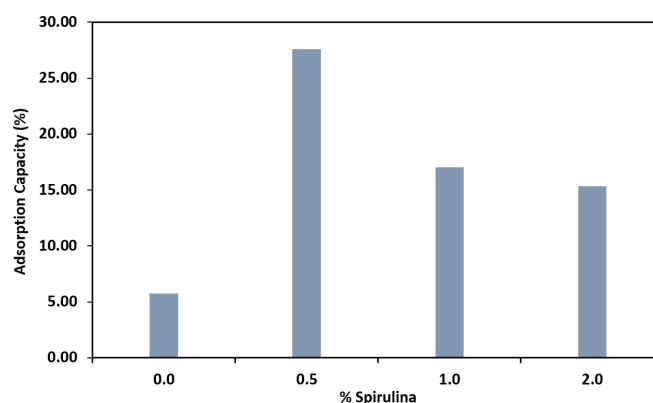
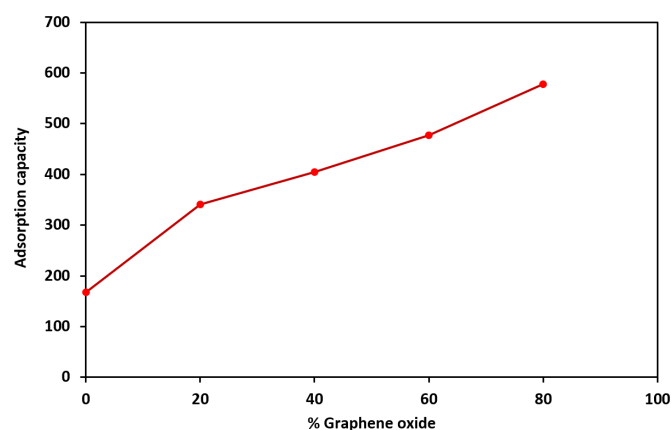
### 3.7. Adsorption study

Hydrogels can be used to remove pollutants from water sources through the adsorption of the pollutant to the hydrogel. By adding nanoparticles to the hydrogel matrix through any of the preparation methods listed previously, the adsorption

capacity can be enhanced because the number of active sites is increased. The adsorption capacity of CMC-Na/PVA hydrogel is 125.94 mg/g, but when CNCs are added to the hydrogel, the adsorption capacity increases to 163.934 mg/g [87]. Similarly, the SA-g-AA/ $\text{TiO}_2$  NC hydrogel is more efficient in the adsorption of methyl violet than SA-g-PAA: 99.6% and 85%, respectively [103]. Xylan-g-/P(AA-co-AM)/GO NC hydrogels, prepared via in-situ polymerization, can adsorb metal ions. The adsorption capacity for each of the three types of metal ions,  $\text{Pd}^{2+}$ ,  $\text{Zn}^{2+}$ , and  $\text{Cd}^{2+}$ , by the xylan-g-/P(AA-co-AM) hydrogels increased after GO was incorporated (Figure 11), which was attributed to the large amount of -OH and -COOH groups in the GO that provide more active sites [104]. When clay nanoparticles are incorporated into the hydrogel matrix, the adsorption capacity of conventional hydrogels also increases as the clay nanoparticles provide a larger number of active sites.

**Table 1.** Change in the methylene blue adsorption capacity for CMT-g-PAM NC hydrogels as a function of silica loading.

Polymer	Adsorption capacity (mg/g)
CMT-g-PAM	72.91
CMT-g-PAM/SiO <sub>2</sub> (0.5%)	89.42
CMT-g-PAM/SiO <sub>2</sub> (1%)	93.37
CMT-g-PAM/SiO <sub>2</sub> (1.5%)	99.76

**Figure 12.** The effect of clay concentration on the degree of adsorption of orange dye at pH = 3.**Figure 13.** The effect of Spirulina loading on Cr<sup>6+</sup> adsorption capacity.**Figure 14.** The increase in methylene blue adsorption capacity of agar hydrogels with increased graphene oxide loading.

The adsorption capabilities of organo-MMT loaded P(NIPAM) hydrogels gradually increase with the clay concentration, but plateaus above 2.5% organo-MMT (Figure 12) [84]. In the case of organo-MMT loaded PVA/AAC hydrogels, however, the adsorption of Cu<sup>2+</sup>, Co<sup>2+</sup>, and Ni<sup>2+</sup> increases significantly with the addition of organo-MMT [105].

From Figure 13, we can see that pure PAAm hydrogel can adsorb modest amounts of Cr<sup>6+</sup> ions. Once Spirulina microalgae, immobilized in MMT, was incorporated into the PAAm hydrogel

matrix, an enhanced adsorption capacity was observed [106]. Clearly, the PAAm NC hydrogel containing 0.5% Spirulina was found to have the highest adsorption capacity. Above 1% spirulina loading in the PAAm hydrogel matrix, metal adsorption decreases and plateaus, which is attributed to the functional groups of the Spirulina and MMT coming close enough to detrimentally interact. Carbon-containing montmorillonite-based (CMMT) NC hydrogels made with cellulose exhibited an increase in their adsorption capacity of methylene

blue over the H<sub>2</sub>SO<sub>4</sub>-MMT precursor. [107]. A PAMPS hydrogel prepared by the polymerization of 2-acrylamido-2-methylpropanesulfonic acid and pectin with *N,N*-methylenebisacrylamide (Pec-g-PAMPS), also used to adsorb methylene blue, showed a maximum adsorption of 62 mg/g. Once the hydrogel was loaded with Ag NPs to form a Pec-g-PAMPS-silver NC hydrogel, the adsorption capacity increased to 89 mg/g [108]. Polyacrylamide grafted carboxymethyl tamarind (CMT-g-PAM) hydrogels have also been investigated for the adsorption of methylene blue, although they exhibit a much lower adsorption capacity of 32 mg/g. When silica is incorporated into the hydrogel matrix, the adsorption capacity increases to 44 mg/g, which, while still low, is a significant increase (Table 1) [109]. An agar/GO aerogel, also used to adsorb methylene blue, had a similar initial adsorption capacity as the CMMT NC hydrogel. However, it exhibited more significant adsorption capacity increases as the GO content increased (Figure 14). This is attributed to the higher number of adsorption sites supplied by the increased number of GO sheets, although the stability of the aerogel decreased with increasing GO concentration [110].

#### 4. Applications

The combination of nanoparticles and hydrogels produces NC hydrogels with a myriad of applications, which are not available from the components alone. The materials used to prepare the NC hydrogel can be strategically chosen to create a hydrogel with specific properties for a chosen application. [47]. Ag NPs are particularly useful for their antimicrobial properties and have been investigated in NC hydrogels to prevent infections in various medical settings [111]. When loaded into a PVA hydrogel matrix, a NC hydrogel is formed, which can release antimicrobial Ag NPs into the wound slowly, maximizing the antimicrobial usefulness of the NPs [112]. Ag NPs were also recently integrated into a guar gum/poly(acrylic acid) hydrogel matrix to form electrically conductive NC hydrogels. Characterization of the prepared silver/guar gum/poly(acrylic acid) NC hydrogels showed that as the concentration of Ag NPs increased, so too did the electrical conductivity. However, as the electrical conductivity increased, the swelling ratio decreased, leading to the conclusion that increasing Ag NP concentrations leads to decreasing swelling ratios. Logically, this means that the Ag NP concentration must be carefully chosen to optimize the resulting NC hydrogel for its chosen application [113]. The high cost of gold has so far prevented the widespread use of Au-NPs in NC hydrogels, though Au-NP-hydrogel composites have shown efficacy in surface plasmon resonance sensors [114] and antibacterial applications [115].

While Ag NPs and Au-NPs are the most common metal NC hydrogels studied, many other metal NPs have been investigated, namely in the fields of catalysis, magnetic components, and environmental nanotechnology. Platinum NPs grown in a bola-amphiphile hydrogel has been shown to be an effective catalyst for the hydrogenation of *p*-nitroaniline [116]. Magnetic cobalt NPs were also used in hydrogels to form a soft and muscle-like magnetic field-driven actuator [117]. Nickel and nickel oxide NPs integrated into PVA hydrogels were responsive to magnetic manipulation and used to remove chemical species from a mixture [118]. A cheap alternative to Ag and Au-NPs for antimicrobial applications was investigated by incorporating copper into poly(ethylene glycol diacrylate) (PEGDA) hydrogel films. The films proved useful as antimicrobial devices but were limited to short-term use due to their irritating effect on skin [119]. Other metal oxide NPs have been investigated for use as antimicrobial surfaces, including titanium and zinc oxides [47].

Non-metallic NPs, including carbon-based materials (GO, nanodots, nanotubes), quantum dots, and silicon, were used to create NC hydrogels with unique functional properties. Si NP

hydrogel composites showed high efficiency for pH-dependent drug release when filled with a medication like doxorubicin [120]. The NIR absorbance of materials like carbon nanotubes [121], GO [122], and melanin [123], when incorporated in hydrogel matrices, make them extremely suitable for photothermal drug delivery. These materials provide synthetic alternatives to remote photothermal systems based on Au- or Ag-NPs.

Polymeric NPs composed of micelles [124], nanogels [125], core-shell particles [126], dendrimers [127], cellulose derivatives [128], and hyperbranched polymers [129] have been developed for many applications. The incorporation of polyamidoamine dendritic NPs into a collagen matrix resulted in an increase in collagen's biological stability [130]. PS NPs have been incorporated into acrylamide and 2-hydroxyethyl methacrylate hydrogels as a filler, which increased the adhesive capabilities and strength of pressure-sensitive adhesive patches [131]. An agarose/alginate hydrogel with polypyrrole NPs was developed for use as an infrared-sensitive drug release system [132]. Na-MMT dispersed in carboxymethyl cellulose-hydroxyethyl cellulose-acrylonitrile-linseed oil polyol (CHAP) hydrogel matrices have proven to be promising for pH-dependent anticancer drug delivery [133]. For the adsorption of textile dyes such as methylene blue [107], crystal violet [86], and heavy metals [105] from industrial waste, nanocomposite hydrogels have proven to be more efficient than conventional hydrogels.

#### 5. Conclusion

Nanocomposite hydrogels are fascinating materials that combine the functionality of nanoparticles with the mechanical properties of hydrogels. The interactions between the individual components result in hydrogels with enhanced physical and chemical properties. With a strategic selection of the nanoparticle and hydrogel type, the functionality and mechanical properties can be predicted and tuned to produce nanomaterials for many applications, particularly in the biomedical and dye adsorption fields. Once the current limitations of nanocomposite hydrogels concerning toxicity, biodegradation, and degree of enhancement of mechanical properties are overcome, these materials have the potential to become useful in practical, everyday applications.

#### Acknowledgement

The authors would like to thank Ashley Tubbs for her guidance in writing this review. The corresponding author is happy with the other authors for collecting the information and data for writing this review.

#### Disclosure statement

Conflict of interests: The authors declare that they have no conflict of interest.

Author contributions: All authors contributed equally to this work.

Ethical approval: All ethical guidelines have been adhered.

#### ORCID

Md. Arif Roman Azady

 <https://orcid.org/0000-0001-9636-552X>

Sony Ahmed

 <https://orcid.org/0000-0002-1432-3957>

Md. Shafiul Islam

 <https://orcid.org/0000-0001-8375-688X>

## References

- [1]. Yang, Y.; Han, S.; Fan, Q.; Ugbolue, S. C. *Text. Res. J.* **2005**, 75 (8), 622–627.
- [2]. Li, S.; Zhang, H.; Feng, J.; Xu, R.; Liu, X. *Desalination* **2011**, 280 (1–3), 95–102.
- [3]. Janovak, L.; Varga, J.; Kemeny, L.; Dekany, I. *Appl. Clay Sci.* **2009**, 43 (2), 260–270.
- [4]. Bahram, M.; Mohseni, N.; Moghtader, M. An Introduction to Hydrogels and Some Recent Applications. In *Emerging Concepts in Analysis and Applications of Hydrogels*; InTech, 2016. <https://www.intechopen.com/books/emerging-concepts-in-analysis-and-applications-of-hydrogels/an-introduction-to-hydrogels-and-some-recent-applications>. (accessed January 10, 2020).
- [5]. Abou Taleb, M. F.; Hegazy, D. E.; Ismail, S. A. *Carbohydr. Polym.* **2012**, 87 (3), 2263–2269.
- [6]. Caló, E.; Khutoryanskiy, V. V. *Eur. Polym. J.* **2015**, 65, 252–267.
- [7]. Wang, H.; Heilshorn, S. C. *Adv. Mater.* **2015**, 27 (25), 3717–3736.
- [8]. Li, J.; Mooney, D. J. *Nat. Rev. Mater.* **2016**, 1 (12), 16071, 1–17.
- [9]. Qin, M.; Sun, M.; Hua, M.; He, X. *Curr. Opin. Solid State Mater. Sci.* **2019**, 23 (1), 13–27.
- [10]. Xue, Z.; Wang, S.; Lin, L.; Chen, L.; Liu, M.; Feng, L.; Jiang, L. *Adv. Mater.* **2011**, 23 (37), 4270–4273.
- [11]. Bohidar, H. B.; Dubin, P.; Osada, Y. *Polymer Gels: Fundamentals and Applications*; American Chemical Society, 2002.
- [12]. Rama Rao, G. V.; Balamurugan, S.; Xu, H.; Xu, Q.; López, G. P. *Chem. Mater.* **2002**, 14 (12), 5075–5080.
- [13]. Guilherme, M. R.; Silva, R.; Girotto, E. M.; Rubira, A. F.; Muniz, E. C. *Polymer (Guildf.)* **2003**, 44 (15), 4213–4219.
- [14]. Liu, Y.; Xie, J.-J.; Zhang, X.-Y. *J. Appl. Polym. Sci.* **2003**, 90 (13), 3481–3487.
- [15]. Ketelson, H. A.; Meadows, D. L.; Stone, R. P. *Colloids Surf. B Biointerfaces* **2005**, 40 (1), 1–9.
- [16]. Bandla, M.; Abbavaram, B. R.; Kokkarchedu, V.; Sadiku, R. E. *Polym. Compos.* **2017**, 38, E16–E23.
- [17]. Boyko, V.; Pich, A.; Lu, Y.; Richter, S.; Arndt, K.-F.; Adler, H.-J. P. *Polymer (Guildf.)* **2003**, 44 (26), 7821–7827.
- [18]. Kuckling, D.; Ivanova, I. G.; Adler, H.-J. P.; Wolff, T. *Polymer (Guildf.)* **2002**, 43 (6), 1813–1820.
- [19]. Vo, C. D.; Kuckling, D.; Adler, H.-J. P.; Schnhoff, M. *Colloid Polym. Sci.* **2002**, 280 (5), 400–409.
- [20]. Zhang, X.-Z.; Zhuo, R.-X. *Macromol. Rapid Commun.* **1999**, 20 (4), 229–231.
- [21]. Serizawa, T.; Wakita, K.; Akashi, M. *Macromolecules* **2002**, 35 (1), 10–12.
- [22]. Zhang, X.-Z.; Yang, Y.-Y.; Chung, T.-S.; Ma, K.-X. *Langmuir* **2001**, 17 (20), 6094–6099.
- [23]. Zhang, X.-Z.; Zhuo, R.-X. *Colloid Polym. Sci.* **1999**, 277 (11), 1079–1082.
- [24]. Van Durme, K.; Van Mele, B.; Loos, W.; Du Prez, F. E. *Polymer (Guildf.)* **2005**, 46 (23), 9851–9862.
- [25]. Zhang, X.-Z.; Zhuo, R.-X. *Eur. Polym. J.* **2000**, 36 (3), 643–645.
- [26]. Bin Imran, A.; Esaki, K.; Gotoh, H.; Seki, T.; Ito, K.; Sakai, Y.; Takeoka, Y. *Nat. Commun.* **2014**, 5 (1), 5124.
- [27]. Sun, J.-Y.; Zhao, X.; Illeperuma, W. R. K.; Chaudhuri, O.; Oh, K. H.; Mooney, D. J.; Vlassak, J. J.; Suo, Z. *Nature* **2012**, 489 (7414), 133–136.
- [28]. Okumura, Y.; Ito, K. *Adv. Mater.* **2001**, 13 (7), 485–487.
- [29]. Merino, S.; Martín, C.; Kostarelos, K.; Prato, M.; Vázquez, E. *ACS Nano* **2015**, 9 (5), 4686–4697.
- [30]. Wu, Y.; Zhou, Z.; Fan, Q.; Chen, L.; Zhu, M. J. *Mater. Chem.* **2009**, 19 (39), 7340–7346.
- [31]. Lin, J.; Xu, S.; Shi, X.; Feng, S.; Wang, J. *Polym. Adv. Technol.* **2009**, 20 (7), 645–649.
- [32]. Tang, Q.; Sun, X.; Li, Q.; Wu, J.; Lin, J.; Huang, M. *E-polymers* **2009**, 9 (1). <https://doi.org/10.1515/epoly.2009.9.1.1087>
- [33]. Fleischmann, C.; Gopez, J.; Lundberg, P.; Ritter, H.; Killops, K. L.; Hawker, C. J.; Klinger, D. *Polym. Chem.* **2015**, 6 (11), 2029–2037.
- [34]. Abdurrahmanoglu, S.; Can, V.; Okay, O. *J. Appl. Polym. Sci.* **2008**, 109 (6), 3714–3724.
- [35]. Mansoori, Y.; Salemi, H. *Polym. Sci. Ser. B* **2015**, 57 (2), 167–179.
- [36]. Chen, T.; Hou, K.; Ren, Q.; Chen, G.; Wei, P.; Zhu, M. *Macromol. Rapid Commun.* **2018**, 39 (21), e1800337.
- [37]. Haraguchi, K.; Takehisa, T. *Adv. Mater.* **2002**, 14 (16), 1120–1124.
- [38]. Liu, R.; Liang, S.; Tang, X.-Z.; Yan, D.; Li, X.; Yu, Z.-Z. *J. Mater. Chem.* **2012**, 22 (28), 14160–14167.
- [39]. Sun, G.; Li, Z.; Liang, R.; Weng, L.-T.; Zhang, L. *Nat. Commun.* **2016**, 7 (1), 12095.
- [40]. Hu, Z.; Chen, G. *Adv. Mater.* **2014**, 26 (34), 5950–5956.
- [41]. Binnemans, K. *Chem. Rev.* **2009**, 109 (9), 4283–4374.
- [42]. Bünzli, J.-C. G. *Chem. Rev.* **2010**, 110 (5), 2729–2755.
- [43]. Liu, F.; Carlos, L. D.; Ferreira, R. A. S.; Rocha, J.; Gaudino, M. C.; Robitzer, M.; Quignard, F. *Biomacromolecules* **2008**, 9 (7), 1945–1950.
- [44]. Qiao, Y.; Lin, Y.; Zhang, S.; Huang, J. *Chemistry* **2011**, 17 (18), 5180–5187.
- [45]. Schexnailder, P.; Schmidt, G. *Colloid Polym. Sci.* **2009**, 287 (1), 1–11.
- [46]. Gaharwar, A. K.; Peppas, N. A.; Khademhosseini, A. *Biotechnol. Bioeng.* **2014**, 111 (3), 441–453.
- [47]. Thoniyot, P.; Tan, M. J.; Karim, A. A.; Young, D. J.; Loh, X. J. *Adv. Sci. (Weinh.)* **2015**, 2 (1–2), 1400010.
- [48]. Lei, Z.; Wang, Q.; Sun, S.; Zhu, W.; Wu, P. *Adv. Mater.* **2017**, 29, 1700321.
- [49]. Zhang, X.; Pint, C. L.; Lee, M. H.; Schubert, B. E.; Jamshidi, A.; Takei, K.; Ko, H.; Gillies, A.; Bardhan, R.; Urban, J. J.; Wu, M.; Fearing, R.; Javey, A. *Nano Lett.* **2011**, 11 (8), 3239–3244.
- [50]. Wang, W.; Chen, J.; Li, M.; Jia, H.; Han, X.; Zhang, J.; Zou, Y.; Tan, B.; Liang, W.; Shang, Y.; Xu, Q.; A. S.; Wang, W.; Mao, J.; Gao, X.; Fan, G.; Liu, W. *ACS Appl. Mater. Interfaces* **2019**, 11 (3), 2880–2890.
- [51]. Van Tran, V.; Park, D.; Lee, Y.-C. *Environ. Sci. Pollut. Res. Int.* **2018**, 25 (25), 24569–24599.
- [52]. Tang, S.; Zeng, Y.; Wang, X. *Polym. Eng. Sci.* **2010**, 50 (11), 2252–2257.
- [53]. Abdullah, Z. W.; Dong, Y.; Davies, I. J.; Barbhuiya, S. *Polym. Plast. Technol. Eng.* **2017**, 56 (12), 1307–1344.
- [54]. Kumar, D.; Jat, S. K.; Khanna, P. K.; Vijayan, N.; Banerjee, S. *Int. J. Green Nanotech.* **2012**, 4 (3), 408–416.
- [55]. Aslam, M.; Kalyar, M. A.; Raza, Z. A. *J. Mater. Sci.: Mater. Electron.* **2017**, 28 (18), 13401–13413.
- [56]. Godovsky, D. Y. Device Applications of Polymer-Nanocomposites. In *Biopolymers · PVA Hydrogels, Anionic Polymerisation Nanocomposites*; Springer Berlin Heidelberg: Berlin, Heidelberg, 2000; pp 163–205.
- [57]. Ruiz-Palmero, C.; Soriano, M. L.; Benítez-Martínez, S.; Valcárcel, M. *Sens. Actuators B Chem.* **2017**, 245, 946–953.
- [58]. Sui, B.; Li, Y.; Yang, B. *Chin. Chem. Lett.* **2020**, 31 (6), 1443–1447.
- [59]. Konwar, A.; Gogoi, N.; Majumdar, G.; Chowdhury, D. *Carbohydr. Polym.* **2015**, 115, 238–245.
- [60]. Martín-Pacheco, A.; Del Río Castillo, A. E.; Martín, C.; Herrero, M. A.; Merino, S.; García Fierro, J. L.; Díez-Barra, E.; Vázquez, E. *ACS Appl. Mater. Interfaces* **2018**, 10 (21), 18192–18201.
- [61]. Shao, H.; Wang, C.-F.; Chen, S.; Xu, C. J. *Polym. Sci. A Polym. Chem.* **2014**, 52 (7), 912–920.
- [62]. Hu, M.; Gu, X.; Hu, Y.; Wang, T.; Huang, J.; Wang, C. *Macromolecules* **2016**, 49 (8), 3174–3183.
- [63]. Guo, J.; Zhou, M.; Yang, C. *Sci. Rep.* **2017**, 7 (1), 7902.
- [64]. Wang, L.; Li, B.; Xu, F.; Li, Y.; Xu, Z.; Wei, D.; Feng, Y.; Wang, Y.; Jia, D.; Zhou, Y. *Biomaterials* **2017**, 145, 192–206.
- [65]. Rezazadeh, B.; Sirousazar, M.; Abbasi-Chianeh, V.; Kheiri, F. *J. Appl. Polym. Sci.* **2020**, 137 (18), 48631.
- [66]. Huang, Q.; Du, C.; Hua, Y.; Zhang, J.; Peng, R.; Yao, X. *BioResources* **2019**, 14, 7134–7147.
- [67]. Liao, G.; Hu, J.; Chen, Z.; Zhang, R.; Wang, G.; Kuang, T. *Front. Chem.* **2018**, 6, 450.
- [68]. Liu, Y.; Gao, T.; Xiao, H.; Guo, W.; Sun, B.; Pei, M.; Zhou, G. *Electrochim. Acta* **2017**, 229, 239–252.
- [69]. Sheng, K.-X.; Xu, Y.-X.; Li, C.; Shi, G.-Q. *New Carbon Mater.* **2011**, 26 (1), 9–15.
- [70]. Cong, H.-P.; Ren, X.-C.; Wang, P.; Yu, S.-H. *ACS Nano* **2012**, 6 (3), 2693–2703.
- [71]. Tungkavet, T.; Seetapan, N.; Pattavarakorn, D.; Sirivat, A. *Polymer (Guildf.)* **2015**, 70, 242–251.
- [72]. Sershen, S. R.; Westcott, S. L.; Halas, N. J.; West, J. L. *Appl. Phys. Lett.* **2002**, 80 (24), 4609–4611.
- [73]. Pardo-Yissar, V.; Gabai, R.; Shipway, A. N.; Bourenko, T.; Willner, I. *Adv. Mater.* **2001**, 13 (17), 1320–1323.
- [74]. Liu, M.; Ishida, Y.; Ebina, Y.; Sasaki, T.; Aida, T. *Nat. Commun.* **2013**, 4 (1), 2029.
- [75]. Khoylou, F.; Naimian, F. *Radiat. Phys. Chem. Oxf. Engl.* **1993** **2009**, 78 (3), 195–198.
- [76]. Ranjha, N. M.; Ayub, G.; Naseem, S.; Ansari, M. T. *J. Mater. Sci. Mater. Med.* **2010**, 21 (10), 2805–2816.
- [77]. Abd Alla, S. G.; Nizam El-Din, H. M.; El-Naggar, A. W. M. *Eur. Polym. J.* **2007**, 43 (7), 2987–2998.
- [78]. Park, H.; Guo, X.; Temenoff, J. S.; Tabata, Y.; Caplan, A. I.; Kasper, F. K.; Mikos, A. G. *Biomacromolecules* **2009**, 10 (3), 541–546.
- [79]. Omidian, H.; Hasherni, S. A.; Askari, F.; Nafisi, S. *Iranian J. Polymer Sci. Tech.* **1994**, 3 (2), 115–119.
- [80]. Tighe, B. J. *Br. Polym. J.* **1986**, 18 (1), 8–13.
- [81]. Mohammadi, S.; Vafaie Sefti, M.; Baghban Salehi, M.; Mousavi Moghadam, A.; Rajaeae, S.; Naderi, H. *Asia-Pac. J. Chem. Eng.* **2015**, 10 (5), 743–753.
- [82]. Aalaie, J.; Vasheghani-Farahani, E.; Rahmatpour, A.; Semsarzadeh, M. A. *Eur. Polym. J.* **2008**, 44 (7), 2024–2031.
- [83]. Wong, R. S. H.; Ashton, M.; Dodou, K. *Pharmaceutics* **2015**, 7 (3), 305–319.
- [84]. Kurecic, M.; Smole, M. S. *Nanocomposites-New Trends and Developments*; IntechOpen, 2012.
- [85]. Sirousazar, M.; Kokabi, M.; Hassan, Z. M.; Bahramian, A. R. *J. Macromol. Sci. Phys.* **2012**, 51 (8), 1583–1595.
- [86]. Hosseinzadeh, H. *Pol. J. Chem. Technol.* **2015**, 17 (2), 70–76.
- [87]. Wang, H.; Li, J.; Ding, N.; Zeng, X.; Tang, X.; Sun, Y.; Lei, T.; Lin, L. *Chem. Eng. J.* **2020**, 386 (124021), 124021.

- [88]. Bakravi, A.; Ahmadian, Y.; Hashemi, H.; Namazi, H. *Adv. Polym. Technol.* **2018**, *37* (7), 2625–2635.
- [89]. Franco, M. K. K. D.; Araújo, D. R. de; Paula, E. de; Cavalcanti, L.; Yokaichiya, F. X-ray Scattering Techniques Applied in the Development of Drug Delivery Systems. In *X-ray Scattering*; InTech, 2017. <https://www.intechopen.com/books/x-ray-scattering/x-ray-scattering-techniques-applied-in-the-development-of-drug-delivery-systems> (accessed January 10, 2020).
- [90]. Liu, M.; Li, W.; Rong, J.; Zhou, C. *Colloid Polym. Sci.* **2012**, *290* (10), 895–905.
- [91]. Kazanskii, K. S.; Dubrovskii, S. A. Chemistry and Physics of “Agricultural” Hydrogels. In *Polyelectrolytes Hydrogels Chromatographic Materials*; Springer Berlin Heidelberg: Berlin, Heidelberg, 1992; pp 97–133.
- [92]. Maitland, G. C. *Curr. Opin. Colloid Interface Sci.* **2000**, *5* (5–6), 301–311.
- [93]. Calvert, P. *Adv. Mater.* **2009**, *21* (7), 743–756.
- [94]. Drury, J. L.; Mooney, D. J. *Biomaterials* **2003**, *24* (24), 4337–4351.
- [95]. Yi, J.-Z.; Zhang, L.-M. *Bioresour. Technol.* **2008**, *99* (7), 2182–2186.
- [96]. Pang, J.; Wu, M.; Liu, X.; Wang, B.; Yang, J.; Xu, F.; Ma, M.; Zhang, X. *Sci. Rep.* **2017**, *7* (1), 13233.
- [97]. Haraguchi, K.; Takehisa, T.; Fan, S. *Macromolecules* **2002**, *35* (27), 10162–10171.
- [98]. Haraguchi, K.; Farnworth, R.; Ohbayashi, A.; Takehisa, T. *Macromolecules* **2003**, *36* (15), 5732–5741.
- [99]. Choi, Y.; Simonsen, J. *J. Nanosci. Nanotechnol.* **2006**, *6* (3), 633–639.
- [100]. Zhou, C.; Wu, Q. *Colloids Surf. B Biointerfaces* **2011**, *84* (1), 155–162.
- [101]. Coats, A. W.; Redfern, J. P. *Analyst* **1963**, *88* (1053), 906–924.
- [102]. Thomas, S.; Thomas, R.; Zachariah, A. K.; Kumar, R. *Thermal and Rheological Measurement Techniques for Nanomaterials Characterization*, 1st ed.; Elsevier, 2017.
- [103]. Thakur, S.; Arotiba, O. *Adsorp. Sci. Technol.* **2018**, *36* (1–2), 458–477.
- [104]. Kong, W.; Chang, M.; Zhang, C.; Liu, X.; He, B.; Ren, J. *Polymers (Basel)* **2019**, *11* (4), 621.
- [105]. Mohsen, M.; 1 Physics Department, Faculty of Science, Ain Shams University, Abbassia, 11566, Cairo, Egypt; Gomaa, E.; Ahmed Mazaid, N.; Mohammed, R. *AIMS Mater. Sci.* **2017**, *4* (5), 1122–1139.
- [106]. Aydinoglu, D.; Akgül, Ö.; Bayram, V.; Şen, S. *Polym. Plast. Technol. Eng.* **2014**, *53* (16), 1706–1722.
- [107]. Tong, D. S.; Wu, C. W.; Adebajo, M. O.; Jin, G. C.; Yu, W. H.; Ji, S. F.; Zhou, C. H. *Appl. Clay Sci.* **2018**, *161*, 256–264.
- [108]. Babaladimath, G.; Badalamoole, V. *Polym. Bull. (Berl.)* **2019**, *76* (8), 4215–4236.
- [109]. Pal, S.; Ghorai, S.; Das, C.; Samrat, S.; Ghosh, A.; Panda, A. B. *Ind. Eng. Chem. Res.* **2012**, *51* (48), 15546–15556.
- [110]. Chen, L.; Li, Y.; Du, Q.; Wang, Z.; Xia, Y.; Yedinak, E.; Lou, J.; Ci, L. *Carbohydr. Polym.* **2017**, *155*, 345–353.
- [111]. Moritz, M.; Geszke-Moritz, M. *Chem. Eng. J.* **2013**, *228*, 596–613.
- [112]. Bhowmick, S.; Koul, V. *Mater. Sci. Eng. C Mater. Biol. Appl.* **2016**, *59*, 109–119.
- [113]. Abdel-Halim, E. S.; Al-Deyab, S. S. *Int. J. Biol. Macromol.* **2014**, *69*, 456–463.
- [114]. Wang, J.; Banerji, S.; Menegazzo, N.; Peng, W.; Zou, Q.; Booksh, K. S. *Talanta* **2011**, *86*, 133–141.
- [115]. Marsich, E.; Travan, A.; Donati, I.; Di Luca, A.; Benincasa, M.; Crosera, M.; Paoletti, S. *Colloids Surf. B Biointerfaces* **2011**, *83* (2), 331–339.
- [116]. Maity, I.; Rasale, D. B.; Das, A. K. *Soft Matter* **2012**, *8* (19), 5301–5308.
- [117]. Fuhrer, R.; Athanassiou, E. K.; Luechinger, N. A.; Stark, W. J. *Small* **2009**, *5* (3), 383–388.
- [118]. Shi, W.; Crews, K.; Chopra, N. *Mater. Technol. (UK)* **2010**, *25* (3–4), 149–157.
- [119]. Cometa, S.; Iatta, R.; Ricci, M. A.; Ferretti, C.; De Giglio, E. *J. Bioact. Compat. Polym.* **2013**, *28* (5), 508–522.
- [120]. Hu, X.; Hao, X.; Wu, Y.; Zhang, J.; Zhang, X.; Wang, P. C.; Zou, G.; Liang, X.-J. *Mater. Chem. B Mater. Biol. Med.* **2013**, *1* (8), 1109–1118.
- [121]. Samanta, S. K.; Pal, A.; Bhattacharya, S.; Rao, C. N. R. *J. Mater. Chem.* **2010**, *20* (33), 6881–6890.
- [122]. Lo, C.-W.; Zhu, D.; Jiang, H. *Soft Matter* **2011**, *7* (12), 5604–5609.
- [123]. Ninh, C.; Cramer, M.; Bettinger, C. J. *Biomater. Sci.* **2014**, *2* (5), 766–774.
- [124]. Moughton, A. O.; Hillmyer, M. A.; Lodge, T. P. *Macromolecules* **2012**, *45* (1), 2–19.
- [125]. Chacko, R. T.; Ventura, J.; Zhuang, J.; Thayumanavan, S. *Adv. Drug Deliv. Rev.* **2012**, *64* (9), 836–851.
- [126]. Li, G. L.; Möhwald, H.; Shchukin, D. G. *Chem. Soc. Rev.* **2013**, *42* (8), 3628–3646.
- [127]. Schlüter, A. D.; Halperin, A.; Kröger, M.; Vlassopoulos, D.; Wegner, G.; Zhang, B. *ACS Macro Lett.* **2014**, *3* (10), 991–998.
- [128]. Mays, J. W. *Macromolecules* **1988**, *21* (11), 3179–3183.
- [129]. Zhang, H.; Patel, A.; Gaharwar, A. K.; Mihaila, S. M.; Iviglia, G.; Mukundan, S.; Bae, H.; Yang, H.; Khademhosseini, A. *Biomacromolecules* **2013**, *14* (5), 1299–1310.
- [130]. Zhong, S.; Yung, L. Y. L. *J. Biomed. Mater. Res. A* **2009**, *91* (1), 114–122.
- [131]. Bait, N.; Grassl, B.; Derail, C.; Benaboura, A. *Soft Matter* **2011**, *7* (5), 2025–2032.
- [132]. Luo, R.-C.; Lim, Z. H.; Li, W.; Shi, P.; Chen, C.-H. *Chem. Commun. (Camb.)* **2014**, *50* (53), 7052–7055.
- [133]. Kouser, R.; Vashist, A.; Zafaryab, M.; Rizvi, M. A.; Ahmad, S. *ACS Omega* **2018**, *3* (11), 15809–15820.



Copyright © 2021 by Authors. This work is published and licensed by Atlanta Publishing House LLC, Atlanta, GA, USA. The full terms of this license are available at <http://www.eurjchem.com/index.php/eurjchem/pages/view/terms> and incorporate the Creative Commons Attribution-Non Commercial (CC BY NC) (International, v4.0) License (<http://creativecommons.org/licenses/by-nc/4.0>). By accessing the work, you hereby accept the Terms. This is an open access article distributed under the terms and conditions of the CC BY NC License, which permits unrestricted non-commercial use, distribution, and reproduction in any medium, provided the original work is properly cited without any further permission from Atlanta Publishing House LLC (European Journal of Chemistry). No use, distribution or reproduction is permitted which does not comply with these terms. Permissions for commercial use of this work beyond the scope of the License (<http://www.eurjchem.com/index.php/eurjchem/pages/view/terms>) are administered by Atlanta Publishing House LLC (European Journal of Chemistry).